Visualization of Plant Cell Walls by Atomic Force Microscopy

Andrew R. Kirby, A. Patrick Gunning, Keith W. Waldron, Victor J. Morris, and Annie Ng
Institute of Food Research, Norwich Laboratory, Norwich Research Park, Colney, Norwich, NR4 7UA England

ABSTRACT Atomic force microscopy has been used to visualize the ultrastructure of hydrated plant cell wall material from prepared apple (*Malus pumila* MILL; Cox orange pippin), water chestnut (*Eleocharis dulcis* L.), potato (*Solanum tuberosum* L.; Bintje), and carrot (*Daucus carota* L.; Amsterdamse bak) parenchyma. Samples of cell wall material in aqueous suspension were deposited onto freshly cleaved mica. Excess water was blotted away and the moist samples were imaged in air at ambient temperature and humidity. The three-dimensional images obtained highlighted the layered structure of the plant cell walls and revealed features interpreted as individual cellulose microfibrils and plasmodesmata.

INTRODUCTION

Scanning probe microscopy is a powerful new biophysical tool for studying biological material (Engel, 1991; Guckenberger et al., 1992; Hansma and Hoh, 1994; Henderson, 1994; Hoh and Hansma, 1992; Lal and John, 1994; Morris, 1994). This technique is capable of achieving a level of resolution normally associated with the technique of electron microscopy (EM), but obtainable under the "native" or "near native" conditions usually associated with light microscopy. Some of the earliest biological objects studied by atomic force microscopy (AFM) were fixed or dried cells (Butt et al., 1990). Cellular material was examined either after air drying onto suitable substrates or after more elaborate sample preparation, such as fixation or critical point drying (Butt et al., 1990; Gould et al., 1990; Hoh and Hansma, 1992; Putman et al., 1993; Radmacher et al., 1992). Fixed cells are robust and AFM images have revealed, in some cases, subsurface cytoskeletal features. Even in living cells it has been possible to image cytoskeletal components (Chang et al. 1993; Fritz et al., 1993; Henderson et al., 1992; Hoh and Hansma, 1992; Parpura et al., 1992, 1993; Schoenenberger and Hoh, 1994). Imaging of subsurface structures may arise either because the outermost membranous structures are malleable and deform following the contours of the inner hard skeletal structure, or because the AFM probe flows through the mobile membrane, feeling the harder skeletal fragment beneath the surface (Henderson, 1994). Most studies have been made on individual cells and there are few studies reported for multicellular tissues. Studies on tissues are usually on material prepared by standard EM methods such as sectioning or preparation of metal replicas (Kordylewski et al., 1994; Ushiki et al., 1994). Perhaps one of the few and certainly one of the earliest studies on living tissue was that reported on the surface of plant leaves (Butt et al., 1990; Gould et al., 1990).

Plant cells contain a polysaccharide skeletal structure external to the plasmalemma (Fig. 1). For the outermost epidermal cells the cell wall is coated with a waxy cuticle. Thus studies on the surface of plant tissue are unlikely to reveal details of the cell wall structure. Even removal of the waxy cuticle may not reveal molecular structure because of the roughness of the tissue surface. In addition, the cell wall structure of the outermost epidermal cells will be atypical of the normal cell wall structure forming an interface between cells within plant tissue. In particular, one would wish to examine the recently synthesized cell wall structures just below, or exterior to, the plasmalemma. With a surface microscopical method such as AFM it is therefore necessary to homogenize the tissue and to extract cell wall fragments for examination.

At present there are considerable data on the chemistry of cell wall polymers (Selvendran, 1983), but less is known about the spatial arrangement of these polysaccharides within the cell wall. The main technique used for ultrastructural studies of cell walls is transmission electron microscopy (TEM). The most recent studies employ the fast freeze, deep etch, rotary shadowing methods developed by Heuser (Heuser, 1981) and applied to plant cell wall material (McCann et al., 1990). These methods are considered preferable to conventional EM techniques because they do not involve chemical fixation or dehydrants and hence are considered to produce images closer to the "in vivo" state of the cell wall.

Currently there are only a few examples of SPM methods being used to study polysaccharides (Morris, 1994; Gunning et al., 1995; Kirby et al., 1995a,b). Most images of polysaccharides have been obtained by EM methods. Usually the samples are rotary shadowed under vacuum and imaged as metal-coated specimens or replicas to reveal molecular size and shape (Stokke et al., 1987; McCann et al., 1990; Wilkins et al., 1993). The detail resolvable in such images is limited by the grain size of the metallic coating. Metal coating has been suggested as a method for immobilizing polysaccharides for imaging by scanning tunneling microscopy (Wilkins et al., 1993). The methodology is

Received for publication 26 June 1995 and in final form 20 November 1995.

Address reprint requests to Dr. Andrew R. Kirby, Institute of Food Research, Norwich Research Park, Colney, Norwich NR4 7UA England. Tel.: 44-01603-255311; Fax: 44-01603-507723; E-mail: andrew.kirby@bbsrc.ac.uk.

0006-3495/96/03/1138/06 $2.00

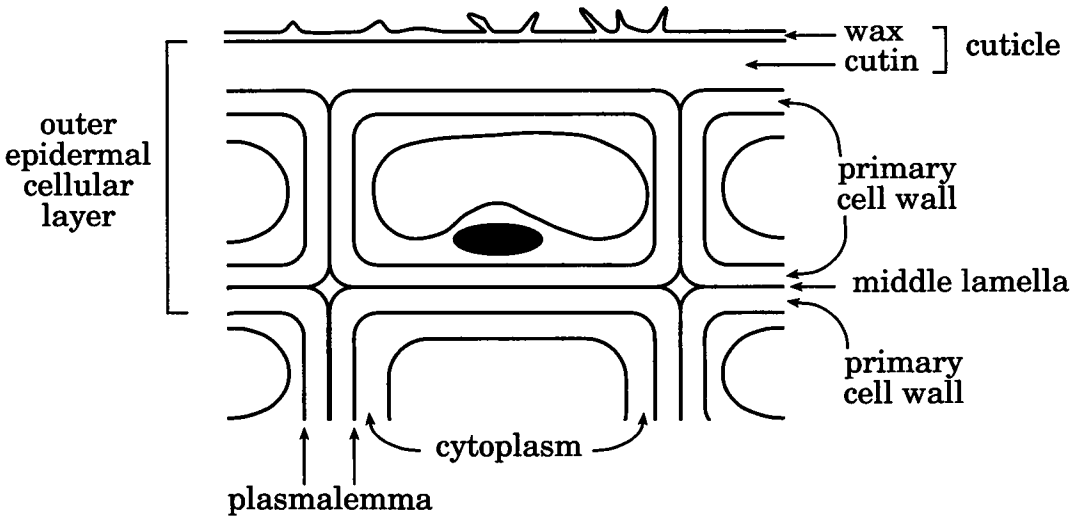

FIGURE 1 Schematic drawing of a section of the cellular structure of the tissue of a plant leaf. The outermost face of mature epidermal cells is protected with a waterproof cutin layer deposited together with an exterior layer of wax. The diagram also illustrates the interfacial cell wall structure connecting cells within the tissue.

simpler than that used for EM studies but there is little, if any, improvement in resolution. For AFM studies of polysaccharides higher resolution images can be obtained by studying uncoated polysaccharides (Gunning et al., 1995; Kirby et al., 1995a,b).

The method for imaging uncoated polysaccharides involves depositing a drop of an aqueous polysaccharide solution onto a freshly cleaved mica surface, allowing the sample to dry in air for a short time, and then imaging under a suitable liquid. The drying step leads to a concentration of the sample. Generally, if the polysaccharide solution concentration is high enough, the polymers are deposited as an entangled network. However, if the polysaccharide exhibits gelling behavior then, during drying, the concentration of the polysaccharide may exceed the critical value required for gelation, resulting in the assembly of the polysaccharides into a gel network. These gel networks are quite resilient and can be imaged by AFM (Gunning et al., 1995) at moderately high imaging forces, which would disrupt or displace individual polysaccharides. This suggested the possibility that AFM could be used to image the molecular structure within hydrated fragments of plant cell walls. The present article demonstrates the feasibility of such studies on plant cell wall material.

MATERIALS AND METHODS

Cell wall material was prepared in the following way. Tissues from freshly harvested organs of Cox orange pippin apples (*Malus pumila* MILL.), water chestnut (*Eleocharis dulcis* L.), Bintje potato (*Solanum tuberosum* L.), and Amsterdamse bak carrot (*Daucus carota* L.) were homogenized in 1.5% (w/v) sodium dodecyl sulfate, 0.05 M Na_2SO_5 (150 ml/1000 g) with an Ystral 7000 homogenizer for 5 min. A few drops of octanol were added to reduce foaming. The homogenate was then filtered through nylon mesh (100 μm), resuspended in 0.5% (w/v) sodium dodecyl sulfate (0.03 M Na_2SO_5), and ball milled for 1–2 h as described elsewhere (Coimbra et al., 1994). This time period is considerably less than the 16 h normally used in the preparation of cell wall material for chemical analysis. The residue was filtered through nylon mesh (60 μm), resuspended in 0.05 M Na_2SO_5 (200–300 ml/100 g) by homogenizing (0.5 min), and refiltered. This procedure was repeated four or five times until the cell contents had been removed (as visualized by light microscopy and, where appropriate, by staining with I_2/KI). The resulting cell wall material was stored as a frozen suspension. Additional experiments were carried out on water chestnut cell wall material to assess the effects of freezing. Fresh purified cell wall material was prepared and imaged by AFM. This material was then frozen (−30°C) for 48 h and then reimaged by AFM.

The following procedure was used to prepare cell wall material for imaging by AFM. The aqueous dispersion of cell wall fragments was applied to the surface of freshly cleaved mica. As the fragments were too large to pipette by conventional methods a modified technique was devised. The aperture of a Gilson pipette was enlarged by making an oblique cut across the end of a pipette tip. In this way relatively large cell wall fragments could be transferred onto the mica surface with ease. The resulting wet deposits were carefully blotted to remove excess liquid, leaving behind large clumps of moist cell wall material. Immediately after this AFM imaging was carried out while the deposit was still visibly moist. This material remained hydrated for periods of several hours. Eventually, overnight, the material dries to a rough dehydrated film. A low-power microscope equipped with a television camera was used to roughly position the AFM probe onto the top of the sample.

AFM imaging was carried out in air in the constant force mode using an ECS (East Coast Scientific, Cambridge, England) instrument. The tips used were the short narrow variety of Nanoprobe cantilevers (Digital Instruments, Santa Barbara, CA) with a nominal force constant of 0.38 Nm^{-1}. Both topographical and "error signal" mode images were collected. Color has been added to the images using 'Photoshop 3.0' (Adobe Systems) to enhance discrimination of fine detail. The color table used progresses linearly from black to bright yellow, according to height in the image.

RESULTS AND DISCUSSIONS

The cell wall fragments as deposited onto the mica contain excess water. This causes problems in imaging. The AFM probe is pulled into the water layer, which then covers the top surface of the cantilever, leading to problems in detecting the motion of the cantilever by deflection of laser light.

One solution would be to submerge the cell wall fragments in water within a liquid cell. Although this would be an ideal solution there are experimental problems: the cell wall fragments float off the mica surface and hence cannot be imaged. In the future it might be possible to devise methods for attaching the cell wall fragments to the mica, thus allowing imaging in water. However, for the present study, it was felt that it would be better to adopt the simplest experimental strategy to assess whether AFM can be used to achieve molecular resolution of plant cell wall architecture. To this end excess water was removed from the samples by blotting and the samples were imaged in air. Because the cell wall fragments are polysaccharide networks they retain water for periods of several hours. Visual inspection of the samples during this period confirmed that they were moist. Water will gradually be lost from the surface of the cell wall fragments and they will eventually dry down to films. This process affects the quality of the AFM images obtained. Over a period of approximately 1 h reproducible high-quality AFM images can be obtained. As the cell wall fragments dry on extended study the quality of the images obtained deteriorates. Eventually (e.g., standing overnight) the samples become too dry and cannot be imaged at all, presumably because of the roughness of the dehydrated film surface.

The preparative procedure used to prepare the cell wall fragments removes the membrane structure, allowing imaging of the newly synthesized region of the skeletal framework of the plant cell wall as viewed from the periplasmic face. The method has been developed from procedures used to prepare cell wall material (CWM) for chemical analysis. The prolonged ball milling in those procedures (>18 h) is extremely disruptive to wall architecture, having been designed to ensure the release of cell contents. The method used in this research study employs ball milling for less than 2 h, ensuring cell rupture, while minimizing wall disruption. Removal of cell contents has been effected by a series of aqueous washes and sieving. While developing methodology for imaging cell walls it was found convenient to store prepared dispersions of cell wall fragment frozen until required. Freeze-thawing of polysaccharides can induce molecular association, and ice crystal growth in tissues can alter structure by inducing large pores. Thus experiments have been performed to assess the effects of freeze-thawing. Water chestnut cell wall samples were imaged from fresh preparations (Fig. 2 *a*) and from samples taken through a representative freeze-thaw stage (Fig. 2 *b*). The images shown in Fig. 2 are "force" or "error signal" mode images. Both show a layer of aligned fibrous structures which, on the basis of shape and size, are taken to be cellulose micro-

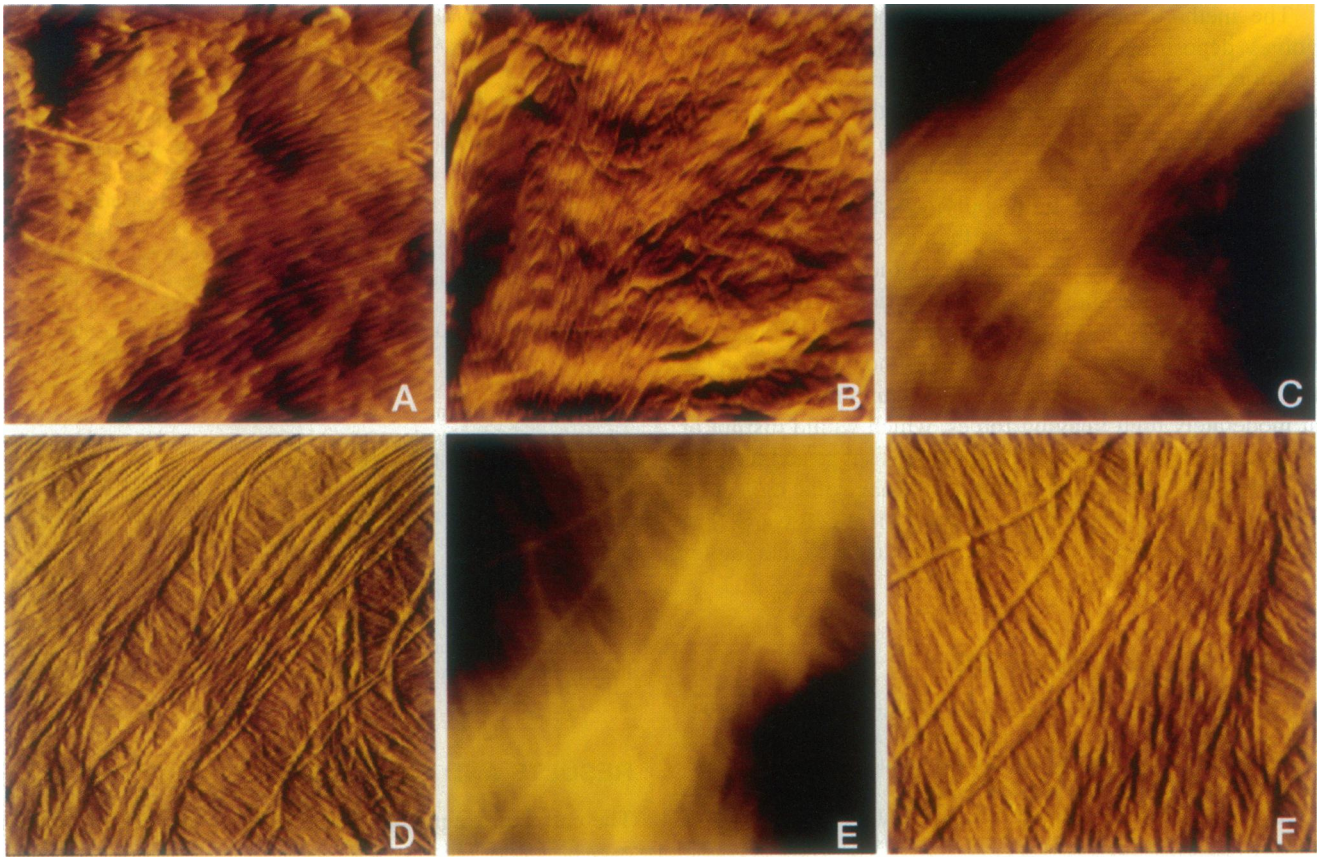

FIGURE 2 AFM images of water chestnut cell walls. Error signal mode images for (*a*) fresh material (scan size 2 × 2 μm) and (*b*) freeze-thawed material (scan size 2 × 2 μm). Matched pairs of topographical (*c*, *e*) and error signal mode (*d*, *f*) images. Image details: (*c*, *d*) scan size 1 × 1 μm, height (*c*), black-to-yellow 0–155 nm. (*e*, *f*) scan size 1 × 1 μm, height (*e*), black-to-yellow 0–104 nm.

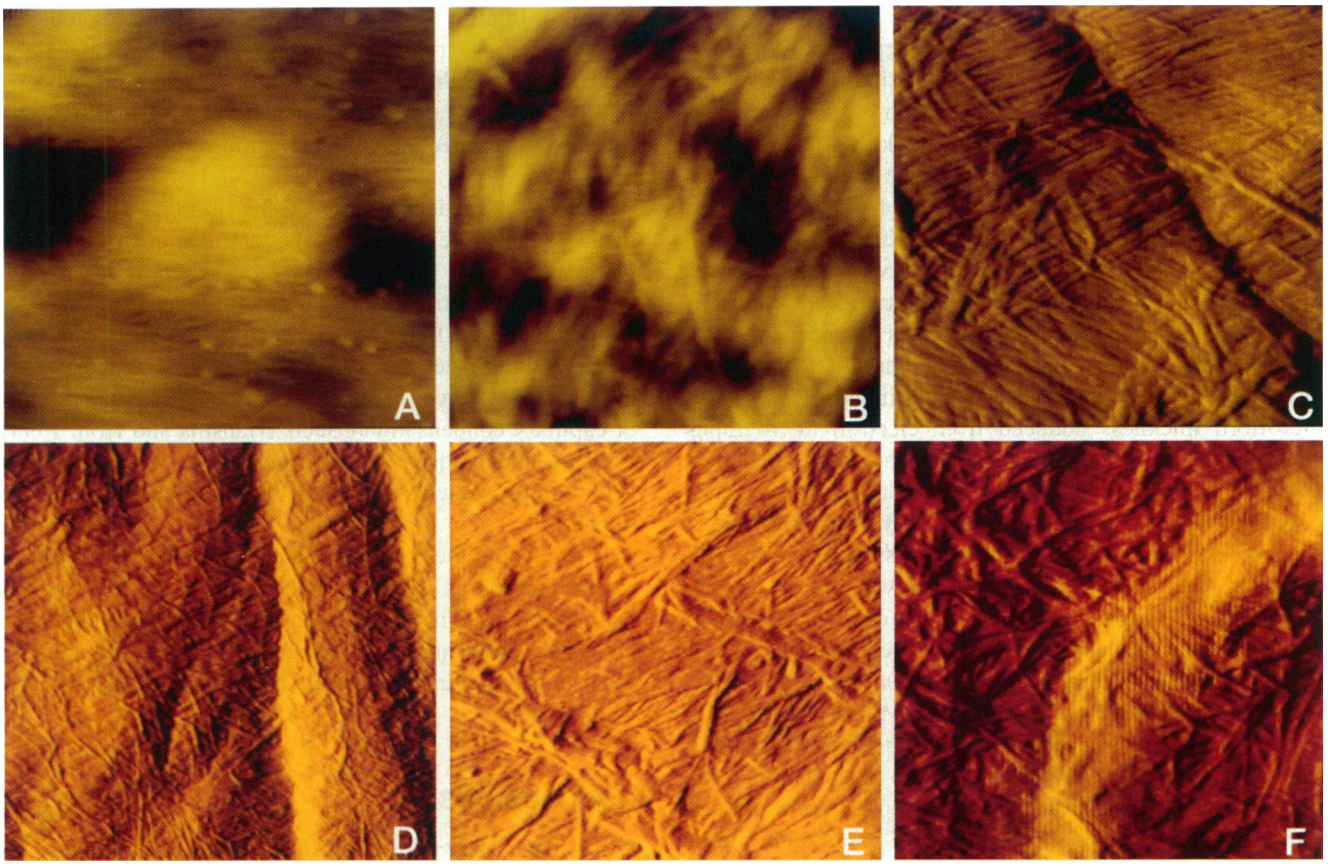

FIGURE 3 AFM images of plant cell walls. (*a*) Topographical image of water chestnut cell wall: scan size 1 × 1 μm, height black-to-yellow 0–85 nm. (*b*) Topographical image of apple cell wall: scan size 1 × 1 μm, height black-to-yellow 0–62 nm. (*c*) Error signal mode image of apple cell wall: scan size 1 × 1 μm. (*d*) Error signal mode image of carrot cell wall: scan size 2.5 × 2.5 μm. (*e*) Error signal mode image of carrot cell wall: scan size 1 × 1 μm. (*f*) Error signal mode image of potato cell wall: scan size 1 × 1 μm.

fibrils. A few isolated fibers are observed on top of the ordered layer. Because the images are of "intact cell walls" the microfibrils observed are likely to be coated with hemicelluloses. The most important observation is that there is no gross change in structure induced by freeze-thawing during sample storage. The images shown in Figs. 2, *a* and *b*, do show minor differences, such as an increase in the fraction and irregularity of the thinner fibrils in the freeze-thawed sample. These small changes are worth further investigation but at present should be viewed with caution, because it is not possible to compare exactly the same areas of the sample before and after freezing. Repeated imaging was not found to cause noticeable distortion or damage to the samples. The remaining images shown in this article are of cell wall fragments that have been stored as a frozen suspension. The ball milling step, although mild, might introduce artifacts into the images. In a preliminary study the effects of ball milling were assessed by maintaining the same experimental conditions but altering the sample concentration. The major effect of this change was to alter the size of the cell wall fragments.

Fig. 2, *c–f*, shows further images of water chestnut cell wall preparations. These images are matched pairs of topographical (Fig. 2, *c* and *e*) and "error signal" mode (Fig. 2, *d* and *f*) images. In these images there is clear evidence for a laminated structure with fibers in different layers showing different orientations. These observations support the common assumption (Roelefson, 1965) that typical cell walls are polylaminate structures. Although the fibers can be seen in both the topographical and error signal mode images, the layering of these fibers is more clearly seen in the error signal mode images. This is due to the roughness of the cell surface. The roughness of the surface is indicated in Fig. 2, *c* and *e*, by the bright and dark regions. Although all of the image contains information on the molecular (fibrous) structure, this high-frequency information is superimposed onto a low-frequency variation representing undulations of the cell wall surface. The eye is only able to perceive the molecular structure in the brighter regions. These topographical images can be improved by a variety of methods that essentially involve eliminating the low-frequency surface undulations. Experimentally this can be achieved by collecting and displaying the "error signal" mode image. The "error signal" is largest whenever the gradient on the surface is largest and emphasizes contrast in the image. A detailed explanation of "error signal" mode imaging is given by Putman et al. (1992). The images shown in Fig. 2, *d* and *f*, confirm the presence of structural information

within the dark regions of the topographical images (Fig. 2, *c* and *e*). The layering of the fibers is very clear in Fig. 2, *d* and *f*. It is noticeable that isolated fibers in the top layer are thicker than fibers that are ordered into aligned arrays or layers. This apparent difference in thickness may be artifactual and due to a reduction in probe broadening when scanning ordered arrays. Such an effect has been observed in studies on aligned polysaccharides (Kirby et al., 1995b). The measurements of fiber thickness within an ordered array will be most representative of the true fiber diameter. For measurements within ordered arrays the fiber diameter appears fairly uniform and on the order of 25 nm. Such values are in good agreement with estimates of cellulose microfibril thickness deduced from electron micrographs (McCann et al., 1990) obtained using the latest methodology. The microfibrillar structure on the uppermost layer is incomplete and open. This is extremely lucky because it permits observation of the multilayered structure of the cell wall. The openness of the uppermost layer may arise from damage during fragmentation. If so, the damage appears to have been restricted almost entirely to the top layer. Loss of water-soluble pectin during fragmentation may also lead to disruption of the cell wall structure. A third possibility is that, as the preparation procedure reveals the newly synthesized region of the cell wall beneath the plasmalemma, the images are of a partially biosynthesized outermost layer. The origins of this open effect are not of paramount importance in the present study. What is important is that the images reveal the multilayered structure. This can only be seen if samples are examined within which the uppermost layer is incompletely synthesized or disrupted.

The images shown in Fig. 2 are typical of over 100 images accumulated for water chestnut cell walls. In one or two images unusual features of the type shown in Fig. 3 *a* were observed. These images showed clusters of small bright objects that appear to protrude above the fibrous layers of the cell wall. It is not possible to identify the exact origin of these features from the present images alone. They could be material remaining from the cytoplasmic contents of the cell. However, very elaborate preparative procedures have been used to ensure removal of such material. The objects appear to be fairly uniform in diameter (43 ± 10 nm) and, as can be seen from Fig. 3 *a*, occur at quite a high density in localized regions of the cell wall. A possible explanation is that these objects are plasmodesmata (Gunning and Robards, 1976). Plasmodesmata are local communication channels between cells. They are formed at the time of the laying down of the cell plate at cytokinesis and are found localized within regions of the primary cell wall called primary pit fields (Brett and Waldron, 1990). This suggestion that the bright objects in Fig. 3 *a* may be plasmodesmata is based solely on a comparison of the AFM image in Fig. 3 *a* with electron micrographs of pit fields containing plasmodesmata (e.g., Alberts et al., 1983).

Water chestnuts are corms. Additional studies have been made on cell wall preparations from a fruit (apple; Fig. 3, *b* and *c*), a root (carrot; Fig. 3, *d* and *e*), and a tuber (potato; Fig. 3 *f*). In all of these samples the AFM images revealed layered fibrous structures. The shape and size of the fibers are consistent with those expected for cellulose microfibrils. In all of the cases studied it has been possible to discern the molecular architecture present within the hydrated cell walls.

These studies demonstrate the feasibility of using AFM methods to probe the molecular architecture of hydrated plant cell walls. The imaging process does not involve fixation, dehydration, or metal coating. Cell walls are examined while still moist and under ambient conditions. Because the images have been obtained in air there will be large adhesive forces between the probe and sample because of capillary condensation effects (Hansma and Hoh, 1994). Imaging under liquid would reduce these factors and may lead to improvements in the level of detail observable in the images.

Even using the present methodology there is clearly scope for probing the development and breakdown of cell wall structures. The use of selective labeling methods coupled with AFM imaging offers the possibility for locating specific carbohydrate or protein components within the cell wall.

CONCLUSIONS

It has been shown that AFM can be used to image the molecular architecture of hydrated plant cell walls after minimal sample preparation. Clearly, AFM represents a new and powerful tool for probing these complex molecular structures. AFM provides resolution comparable to that of the latest EM methods, but with the great advantage of studying hydrated cell wall samples under ambient conditions. Furthermore, AFM has potential for improvement in the resolution of observable detail.

The authors wish to thank Paul A. Gunning for printing the figures used in this article.

Research at IFR was sponsored by the BBSRC.

REFERENCES

Alberts, B., D. Bray, J. Lewis, M. Raff, K. Roberts, and J. D. Watson. 1983. Special features of plant cells. *In* Molecular Biology of the Cell. Garland Publishing, New York and London. 1099–1146.

Brett, C., and K. W. Waldron. 1990. Physiology and biochemistry of plant cell walls. *In* Topics in Plant Physiology, M. Black and J. Chapman, series editors. Unwin Hyman, London. 1–196.

Butt, H. J., E. K. Wolff, S. A. Gould, N. B. Dixon, C. M. Peterson, and P. K. Hansma. 1990. Imaging cells with the atomic force microscope. *J. Struct. Biol.* 105:54–61.

Chang, L., T. Kious, M. Morgancioglu, D. Keller, and J. Pfeifer. 1993. Cytoskeleton of living, unstained cells imaged by scanning force microscopy. *Biophys. J.* 64:1282–86.

Coimbra, M. A., K. W. Waldron, and R. R. Selvendran. 1994. Isolation and characterisation of cell wall polymers for olive pulp (*Olea europaea* L). *Carbohydr. Res.* 252:245–262.

Engel, E. 1991. Biologication applications of scanning probe microscopes. *Annu. Rev. Biophys. Biophys. Chem.* 20:79–108.

Fritz, M., M. Radmacher, and H. E. Gaub. 1993. In vitro activation of human platelets triggered and probed by atomic force microscopy. *Exp. Cell. Res.* 205:187–190.

Gould, S. A. C., B. Drake, C. B. Prater, A. L. Weisshorn, S. Manne, H. G. Hansma, P. K. Hansma, J. Massie, M. Longmire, V. Elings, B. D. Northern, B. Makergee, C. M. Peterson, W. Stoeckenius, T. R. Albrecht, and C. F. Quate. 1990. From atoms to integrated circuit chips, blood cells, and bacteria with the atomic force microscope. *J. Vac. Sci. Technol. A.* 8:369–373.

Guckenberger, R., T. Hartman, W. Weigräbe, and W. Baumeister. 1992. The scanning tunnelling microscope in biology. *In* Scanning Tunnelling Microscopy II. R. Wiesendanger and H-J. Güntherodt, editors. Springer Verlag, Berlin. 51–98.

Gunning, A. P., A. R. Kirby, V. J. Morris, B. Wells, and B. E. Brooker. 1995. Imaging bacterial polysaccharides with AFM. *Polym. Bull.* 34: 615–619.

Gunning, B. E. S., and A. W. Robards, editors. 1976. Plasmodesmata in higher plants. *In* Intercellular communication of plants: studies on plasmodesmata. Springer, Berlin. 16–57.

Hansma, H. G., and J. H. Hoh. 1994. Biomolecular imaging with the atomic force microscope. *Annu Rev. Biophys. Biomol. Struct.* 23: 115–139.

Henderson, E. 1994. Imaging of living cells by atomic force microscopy. *Prog. Surface Sci.* 46:39–60.

Henderson, E., P. G. Haydon, and D. S. Sakaguchi. 1992. Actin filament dynamics in living glial cells imaged by atomic force microscopy. *Science.* 257:1944–1946.

Heuser, J. 1981. Preparing biological samples for stereo microscopy by the quick freeze, deep etch, rotary replication technique. *Methods Cell. Biol.* 22:97–122.

Hoh, J. H., and P. K. Hansma. 1992. Atomic force microscopy for high-resolution imaging in cell biology. *Trends Cell Biol.* 2:208–213.

Kirby, A. R., A. P. Gunning, and V. J. Morris. 1995a. Imaging xanthan gum by atomic force microscopy. *Carbohydr. Res.* 267:161–166.

Kirby, A. R., A. P. Gunning, V. J. Morris, and M. J. Ridout. 1995b. Observation of the helical structure of the bacterial polysaccharide acetan by atomic force microscopy. *Biophys. J.* 68:359–362.

Kordylewski, L., D. Saner, and R. Lal. 1994. Atomic force microscopy of freeze fracture replicas of rat atrial tissue. *J. Microsc.* 173: 173–181.

Lal, R., and S. A. John. 1994. Biological applications of atomic force microscopy. *Am. J. Physiol.* 266(*Cell Physiol.* 35):C1–C21.

McCann, M. C., B. Wells, and K. Roberts. 1990. Direct visualisation of crosslinks in the primary cell wall. *J. Cell. Sci.* 96:323–334.

Morris, V. J. 1994. Biological applications of scanning probe microscopies. *Prog. Biophys. Mol. Biol.* 61:131–185.

Parpura, V., P. G. Haydon, and E. Henderson. 1993. Three-dimensional imaging of living neurons and glia with the atomic force microscope. *J. Cell Sci.* 104:427–432.

Parpura, V., P. G. Haydon, D. S. Sakaguchi, and E. Henderson. 1992. Atomic force microscopy and manipulation of living glial cells. *J. Vac. Sci. Technol. A.* 11:773–775.

Putman, C. A. J., B. G. de Grooth, P. K. Hansma, N. F. van Hulst, and J. Greve. 1993. *Ultramicroscopy.* 48:177–182.

Putman, C. A. J., K. O. van der Werf, B. G. de Grooth, N. F. van Hulst, J. Greve, and P. K. Hansma. 1992. A new imaging mode in atomic force microscopy based on the error signal. *SPIE Scanning Probe Microsc.* 1693:198–204.

Radmacher, M., R. W. Tillman, M. Fritz, and H. E. Gaub. 1992. From molecules to cells: imaging soft samples with the atomic force microscope. *Science.* 257:1900–1905.

Roelefson, P. A. 1965. Ultrastructure of the wall of growing cells and its relation to the direction of growth. *Adv. Bot. Res.* 2:69–149.

Schoenenberger, C-A., and J. H. Hoh. 1994. Slow cellular dynamics in MDCK and R5 cells monitored by time lapse atomic force microscopy. *Biophys. J.* 67:929–936.

Selvendran, R. R. 1983. The chemistry of plant cell walls. *In* Dietary fiber. G. G. Birch and K. J. Parker, editors. Applied Science Publishers, London. 95–147.

Stokke, B. T., A. Elgsaeter, G. Skjäk-Braek, and O. Smidsrød. 1987. The molecular size and shape of xanthan, xylinum, bronchial mucin, alginate and amylose as revealed by electron microscopy. *Carbohydr. Res.* 160: 13–28.

Ushiki, T., M. Shigeno, and K. Abe. 1994. Atomic force microscopy of embedment-free sections of cells and tissues. *Arch. Histol. Cytol.* 57: 427–432.

Wilkins, M. J., M. C. Davies, D. E. Jackson, J. R. Mitchell, C. J. Roberts, B. T. Stokke, and S. J. B. Tendler. 1993. Comparison of scanning tunnelling microscopy and transmission electron microscopy image data of a microbial polysaccharide. *Ultramicroscopy.* 48:197–207.